Mobility Performance of Macrocell-Assisted Small Cells in Manhattan Model

Murat Karabacak*, Dexin Wang†, Hiroyuki Ishii‡, and Huseyin Arslan*§
*Department of Electrical Engineering University of South Florida, Tampa, FL, 33620
†Department of Electrical and Computer Engineering, Colorado State University, Fort Collins, CO 80523
‡DOCOMO Innovations Inc., 3240 Hillview Avenue, Palo Alto, CA, 94304
§Department of Electrical Engineering of Istanbul Medipol University, Istanbul, Turkey
Email: murat@mail.usf.edu, dxwang@engr.colostate.edu, ishii@docomoinnovations.com, and arslan@usf.edu.

***Abstract*—Macrocell-assisted small cell concepts, such as Phantom cell concept and soft cell concept, have been proposed previously for interference management, flexible cell planning, and energy saving in dense small cell deployments. These concepts require macrocell involvement to improve links between small cell and user. Since target implementation areas of the concepts are crowded urban areas (e.g. downtown New York City) to satisfy the data need, more realistic simulations are needed to be implemented compared to conventional evaluations. In this paper, as a new approach to urban area LTE simulations, Manhattan grid layout is presented and implemented for mobility performance of Macrocell-assisted small Cell concept. The results show that the macrocell involvement to improve mobility performance gives a great advantage compared to using the conventional mobility solution for dense small cell deployments.**

***Index Terms*: Manhattan grid layout, Small cell, Mobility.**

I. Introduction

Tremendous development on mobile devices increased their requirements from wireless networks with advanced applications, e.g. high definition video conference, cloud computing/storage. These requirements, e.g. high data rate, low delay, drive wireless technology to develop further and to work efficiently. Small cell network is a good candidate to provide the requirements in the future [1]. 3rd generation partnership project (3GPP) has initialized a workshop on Long Term Evolution (LTE) Release 12 to clarify a path to future technologies [2]. Among the various candidate technologies, enhanced small cells attract interest from the majority of companies. 3GPP also released a technical report on the scenarios and requirements of small cell enhancement [3].

Low power short range cell deployments under macrocell coverage have been proposed in the literature to increase total system capacity. In [4], street micro cells are presented, and their signal propagation is investigated. In [1], current problems of small cell deployments and research areas have been discussed. Despite their capability to provide high system capacity, small cells have mobility and interference problems. The deployment of small cells will result in serious interference with neighbor cells (macrocells in co-channel deployments and small cells in small cell dedicated carrier deployments) because of the frequently repeated usage of resources. Also, when user equipment (UE) moves through the network, dense small cells (more than 10 small cells per macro cell) can increase the number of handovers (HOs) and HO failures compared to conventional macrocell deployments. This significantly increases cell planning, management, and optimization efforts due to a large number of HO points.

To improve interference management, flexible cell planning, and energy saving, macrocell-assisted small cell concepts, such as Phantom Cell and soft cell are proposed in the literature. In [5], the soft small cells are part of the macrocell and share the same system information with the macro cell. The control signaling can be transmitted from the macrocell and the small cell simultaneously, and this results in an improved signal-to-interference-plus-noise ratio (SINR) through an over-the-air signal combination. In the Phantom Cells concept [6], a massive number of small cells using higher frequency band are deployed. The small cells only handle data traffic, and the macrocells handle all the control signaling. In both soft cell and Phantom Cell conceptions, there is macrocell involvement to improve the link between the small cell and its user. Since dense small cell networks can provide high data rates, these concepts are good candidates to be implemented in crowded urban areas (e.g. downtown New York City). Therefore, the Manhattan grid mobility model, which is widely used for urban areas, is suitable to implement realistic simulations for this concept [7], [8]. In this paper, The Manhattan grid model is used to implement more realistic scenarios in LTE simulations. Macrocell performance is investigated in the simulator, and the results are interpreted for small cell mobility.

Our main contribution consists of two parts. First, we improve the current LTE simulator for macrocells by incorporating the Manhattan grid mobility model. The Manhattan grid is seamlessly built upon the conventional hexagonal cell layout. Macrocell deployment and UE movement are also specified. Path loss and shadow fading calculation for cells are also elaborated. Secondly, the impact of UE mobility and macrocell location on HO failure and HO rate are thoroughly studied. The simulation results show that macrocell performance highly depends on relative location of neighboring cells and buildings. To improve performance, line-of-site (LOS) to non-line-of-site (NLOS) transitions at the cell borders should be avoided while deploying macrocells.

978-1-4799-4482-8/14/$31.00 ©2014 IEEE

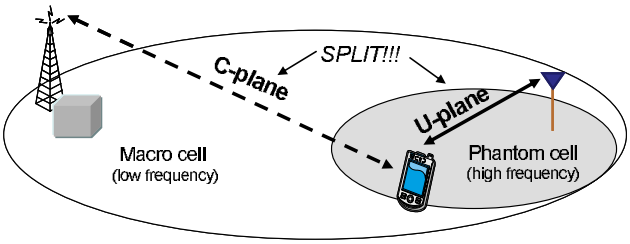

Fig. 1. Phantom cell C-plane/U-plane split

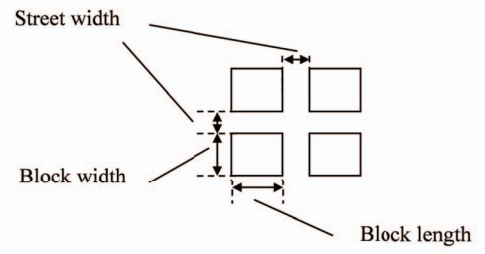

Fig. 2. Manhattan grid layout

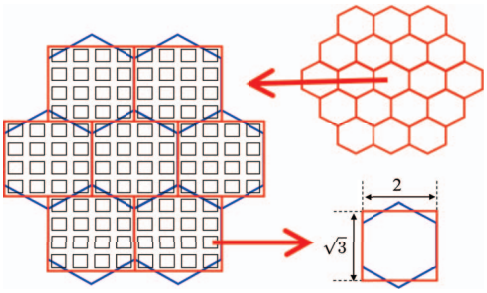

Fig. 3. Macrocell deployment to the corner of buildings

II. Macrocell-Assisted Small Cell Concept

Macrocell-assisted small cells, called Phantom Cells are proposed in [6] for capacity problem in high-traffic outdoor environments. In the Macrocell-assisted small Cell concept, the C-plane/U-plane are split as shown in Fig. 1. One major advantage for this configuration is the possibility of offering substantial capacity increase to an existing network at the same time exploiting the reliable coverage and mobility performance of the macrocell layer. In the proposed architecture, macrocell-assisted small cells are allocated with higher frequency bands while the macrocells keep the existing band. Therefore, the C/U-plane split configuration allows for high capacity connection with U-plane through the small cell (with more bandwidth), while the C-plane is maintained by a more reliable macrocell layer. This configuration also allows operators to deploy a small number of small cells in a sparse manner to boost the user experience at some specific high-traffic spots, which is the case for the initial dense small cell deployment. Since the macrocell layer keeps the reliable coverage and performance, fine cell planning, configuration, and optimization efforts are not required in the small cell layer. For example the operators do not need to worry about the coverage holes any more in the small cell layer. Furthermore, the total capacity can linearly increase as the operators increase the number of cells. This easy-upgrade characteristic is very important in terms of practical system development especially for higher frequency bands, since achieving conventional full cellular coverage is very costly, bothersome, and almost impossible due to poor propagation characteristic at high frequency.

III. System Model

Manhattan grid layout and mobility model is assumed to investigate mobility in realistic downtown scenario. The streets and the buildings are organized as in Fig. 2. Table I shows a set of values for block parameters with 500m inter-site distance (ISD) of macrocells. The block length-to-width ratio is chosen as $\sqrt{3}/2$ to fit the layout on hexagonal layout as in Fig. 3. The model details are given in the following subsections.

TABLE I
Block size and street width

Items	Description
ISD of macro eNBs	500 m
Block length	110 m
Block width	$\approx$ 93.3 m
Street width	15 m

A. Macrocell deployment

To implement the Manhattan model, the conventional hexagonal cell layout has been fit onto Manhattan blocks. Figure 3 gives a Manhattan grid layout for macrocell deployment, when the macrocells are located at the corner of building (at the intersection). Macrocells are uniformly deployed to fixed locations in a 19-cell cluster area with each of the macrocells containing 16 Manhattan blocks. The layout also wrapped around to provide continuity.

To analyze different deployment options macrocells can be also located on 4 different locations. Figure 4 shows possible locations for macrocells. For each option, whole 19-cell grid has been shifted to desired location.

B. User deployment and Mobility

Users are randomly confined to streets with uniform distribution. There is no user in the buildings. Users can move in horizontal or vertical directions. At the intersections, UE chooses a direction to move. The probability of going straight is 0.5 and taking a left or right is 0.25 each. Two speed options are implemented for users. To simulate pedestrian and vehicular mobility, 3 km/h and 50 km/h speeds are chosen as user speed, respectively.

C. Signal Propagation

The effects of terrestrial environment on signal propagation can be classified into three types, i.e., the path loss, slow fading caused by shadowing from obstacles, and fast fading caused by multipath effects. In this subsection, generation of path loss and shadowing in the Manhattan grid is described.

In the Manhattan grid, there are two conditions for the relative position between UE and the Macro cell, i.e., LOS, NLOS that affect the distance loss. Figs. 4 shows assumed

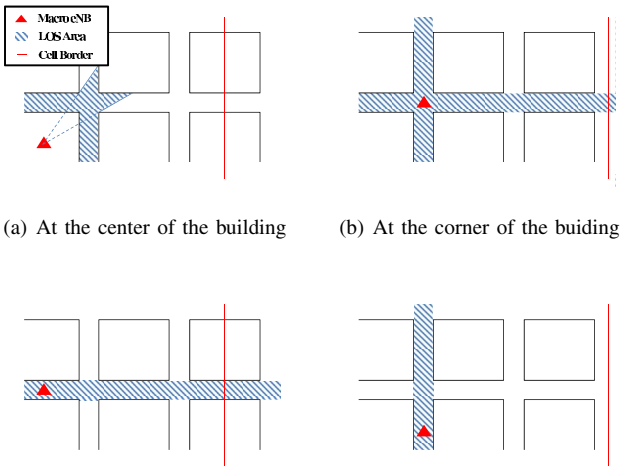

(a) At the center of the building (b) At the corner of the buiding

(c) At the north of the building (d) At the East of the building

Fig. 4. Macrocell locations

LOS and NLOS regions for different Macrocell locations. The path loss formulas for the LOS condition and the NLOS condition are given in the urban macro (UMa) model (Table A1-2 in [9]).

In urban areas, shadow fading has the log-normal distribution, and changes slowly over the period of use. When user moves, shadow fading has to be updated according to the autocorrelation between shadow fading at the current user position and the next user position. Shadow fading is generated and updated using the following steps:

1) N independent normal distributed random variables are created, i.e., $\boldsymbol{x} = [x_1, x_2, \ldots, x_N]$, where N is the number of cells, $x_i \sim \mathcal{N}(0,1),\ i = 1, 2, \ldots, N$.
2) The cross-correlation matrix Γ is constructed as follows:

$$\Gamma = \begin{bmatrix} 1 & \rho_{12} & \cdots & \rho_{1N} \\ \rho_{21} & 1 & \cdots & \rho_{2N} \\ \vdots & \vdots & \ddots & \vdots \\ \rho_{N1} & \rho_{N2} & \cdots & 1 \end{bmatrix}, \quad (1)$$

where $\rho_{ij} = 0.5$ $(i \neq j)$ is the correlation coefficient of the shadow fading between the radio links i and j. Since Γ is a symmetric positive definite matrix, it can be decomposed into a lower and upper triangular matrix by Cholesky decomposition technique, i.e., $\Gamma = \boldsymbol{C}^T\boldsymbol{C}$ and $\boldsymbol{C}$ is an upper triangular matrix.
3) Shadow fading standard deviation is constructed in vector $\Sigma = [\sigma_1, \sigma_2, \ldots, \sigma_N]$, where σ_i is the shadow fading standard deviation at link $i, i = 1, 2, \ldots, N$. In UMa model (Table A1-2 in [9]), the standard deviation is 4 for the LOS condition and 6 for the NLOS condition. Let $\boldsymbol{y} = [y_1, y_2, \ldots, y_N] = \boldsymbol{x}\boldsymbol{C}\text{diag}(\Sigma)$. Then, y_i will be the cross-correlated log-normal shadow fading component for radio link i.
4) When UE moves, the shadow fading components have to be updated. Let $\boldsymbol{x}$ be the independent log-normal vector at the current position obtained in step 1) and $\overline{\boldsymbol{x}}$ be the one at the future position, which is Δd away from the current position. According to the Gudmundson autocorrelation model, the correlation between $\boldsymbol{x}$ and $\overline{\boldsymbol{x}}$ is $\mathbb{E}[\boldsymbol{x}^T\overline{\boldsymbol{x}}] = \text{diag}([\tau_1, \tau_2, \ldots, \tau_N])$, where

$$\tau_i = e^{-\frac{|\Delta d|}{D_i}}, i = 1, 2, \ldots, N. \quad (2)$$

According to the UMa model, $D_i = 37$ m if link i is LOS and $D_i = 50$ m if link i is NLOS (TABLE A1-7 in [9]). Then, the update formula for ith component of $\overline{\boldsymbol{x}}$ is $\overline{x}_i = \tau_i * x_i + \sqrt{1-\tau_i^2} * z_i$, where $z_i \sim \mathcal{N}(0,1)$ is independent of x_i. $\overline{x}_i$ will also be normally distributed with mean 0 and variance 1.
5) The cross-correlated log-normal shadow fading vector $\boldsymbol{y}$ at the future position is updated to be $\overline{\boldsymbol{y}} = \overline{\boldsymbol{x}}\boldsymbol{C}\text{diag}(\Sigma)$.
6) Iterate over steps 4) and 5) throughout the simulation.

TABLE II
PARAMETERS FOR MOBILITY PERFORMANCE EVALUATION

Items	Description
Traffic load	100%
Multipath channel model	Vehicular A
RSRP Measurement bandwidth	25 resource blocks
L1 measurement period	200 msec (5 samples)
Handover preparation (decision) delay	40 ms
Handover execution time	40 ms
SINR threshold for HO failure	-8 dB
Time-to-trigger	160 msec
A3 offset	3 dB

IV. PERFORMANCE EVALUATION

This section presents mobility results for the Manhattan grid mobility model with urban macrocells.

A. Simulation setup

Table A1-2 in [9] is used as basic simulation settings. Additionally, Table II shows mobility parameters implemented in the simulations. In order to simulate and analyze the infinite cellular network using only one macrocell cluster, the wrap-around model in [10] is utilized. SINR and HO rate are used as the performance metric. Also, SINR just before the HO command is sent, is observed to investigate HO failure. As a tentative failure threshold -8 dB SINR is used to find out failure rate. Since SINR before HO is the last SINR value that user sees, it also shows the minimum SINR.

B. Effect of Macrocell Location

In Fig. 5, cumulative distribution function (CDF) of SINR just before the HO is shown for different locations of macrocell at 50 km/h user speed. As it can be seen from the figure, while macrocells are located at the center or at the North, HO failure rate is about 3%. However, when the macrocells are located at the corner or at the East, HO failure rate increases up to 25%. The main reason for that difference can be explained by LOS to NLOS change at the border of a cell as shown in Fig. 6. For corner and East location cases, when UE makes a turn towards the target cell, LOS/NLOS condition changes and the received signal power from source cell drops, dramatically.

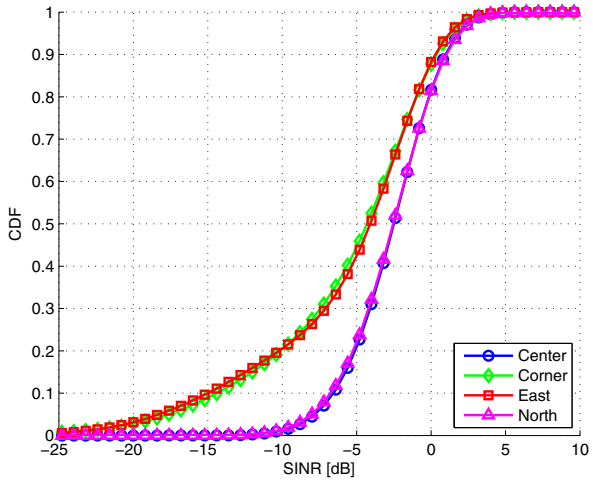

Fig. 5. CDF of SINR Before handover for 50km/h

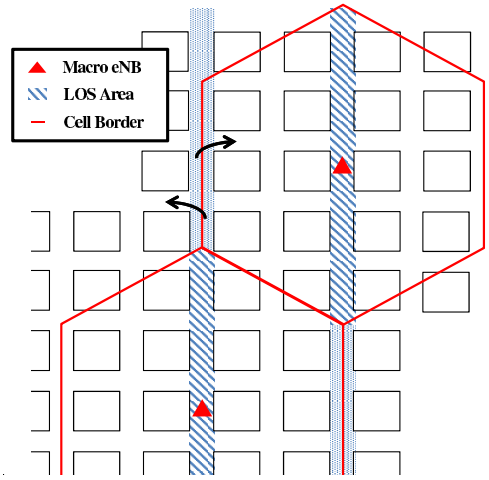

Fig. 6. Handover location

When macrocell is located at the center, LOS condition only occurs at the center area as seen in Fig. 4(a). Therefore, sudden signal level drop at cell boarder does not occur for center case. However, in the North side location case, when the LOS to NLOS change happens at the border, it happens for both target cell and the source cell. Therefore, interference and signal power level drop with similar rates which does not affect the mobility performance.

In summary, macrocell location, more specifically where the LOS/NLOS condition change occur, affects the mobility performance in Manhattan grid model. That is, if the LOS/ NLOS transitions occur in HO areas, the HO performance is degraded due to dramatic change on signal levels for the source cell and target cell. It is noted that macrocells are more likely to be deployed at the center of the building (Fig. 4(a)), but the other cases (Figs. 4(b), 4(c), 4(d)) can also be observed in actual deployments. The location based issues can be mitigated in a case-by-case manner for cell optimization.

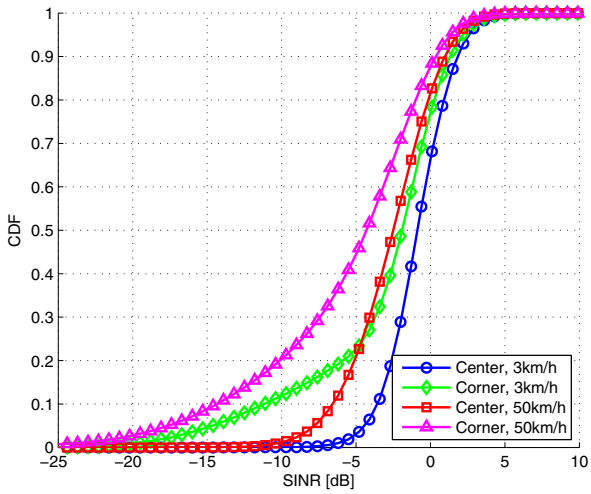

Fig. 7. CDF of SINR Before handover for different speeds

For instance, HO points can be shifted by cell-specific HO offset or cell coverage adjustment by antenna tilting to change HO area to avoid possible LOS to NLOS transitions during HO. These problems caused by LOS/NLOS condition change can be solved with better network planning and optimization. However, since small cells are deployed in large numbers and randomly, this kind of effort can require more operational cost for small cells compared to macrocells. Therefore, macrocell-assisted mobility management gains an interest to reduce operational cost to provide good HO performance.

C. Effect of User speed

In Fig. 7, CDF of SINR just before the HO is shown for different speeds, when macrocell is located at the center or at the corner. As it can be seen from the figure, UE speed has a significant impact on HO performance. When UE speed drops to 3 km/h, HO failure rate is also drops from 3% to 0.1% and from 25% to 14% compared to 50 km/h for center and corner locations, respectively.

D. Overall system performance

In Fig. 8 and Fig. 9, CDF plots of SINR for whole coverage area are shown for user speed 3 km/h and 50 km/h, respectively. The figures indicate that the minimum user SINR is higher than -5 dB, i.e. there are no coverage holes, in all the cases. It can also be seen that the median user SINR (i.e. 50%-tile user) is around 6-7 dB for different locations. It indicates that location of macrocell does not affect overall SINR performance.

E. Comparison between macrocell deployment and small cell deployment

Table III shows a summary of HO performance results for macrocell deployment in Manhattan model and compares them with dense small cell deployments results. In the table HO rate, HO failure rate and as a combination of these two,

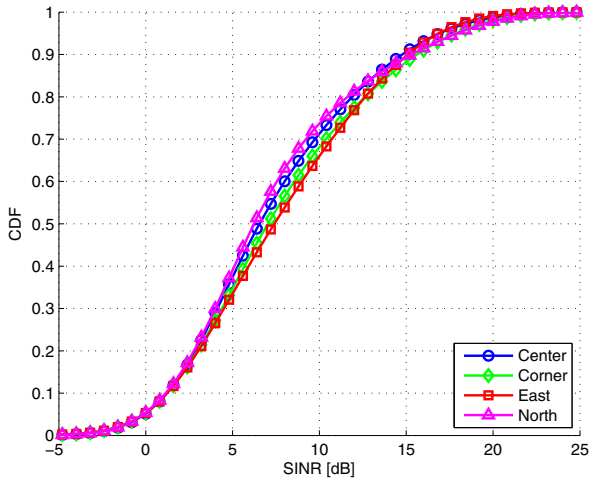

Fig. 8. CDF of SINR for 3 km/h

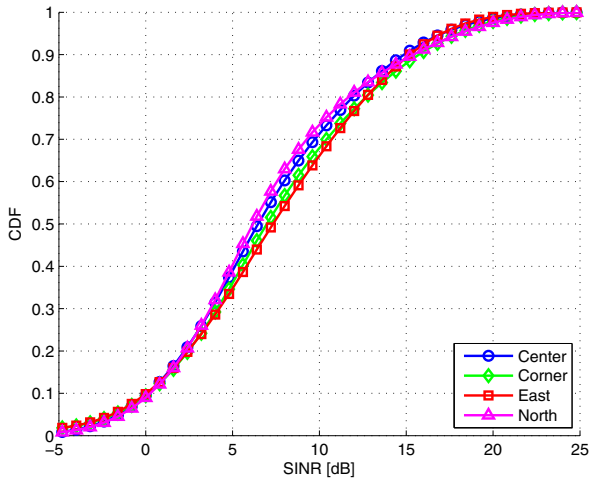

Fig. 9. CDF of SINR for 50km/h

handover failure in time, are given for 4 different cases of macrocell deployment and for 2 different scenarios of small cell deployment. The combination, handover failure, can be seen as connection loss rate because of mobility and this loss requires users to re-establish connection with the network. When macrocell and small cell deployments are compared for 50 km/h user speed, the handover rate is a little more than doubled. This may be acceptable for some networks. However, connection loss rate for small cells is more than 4 times and more than 30 times compared to macrocells located to center and to corner, respectively. These results show the importance of macrocell cooperation for mobility performance as it is introduced in [6].

V. Conclusions

Macrocell cooperation is expected to be implemented to improve interference and mobility performance in dense small cells which are candidate solution for high data rate demanding urban areas. Therefore, by implementing Manhattan grid layout, capability of macrocells to support small cell mobility has been investigated for downtown environment of crowded cities. Macrocells are placed on different locations to compare its effects. The results show that without a macrocell support, dense small cells would require at least 4 times more reconnection load because of the mobility problems. Compared to best case macrocell deployment this load requirement goes up to 30 times more. The results also show that there are location related problems for Manhattan model due to LOS to NLOS transitions in HO area. These issues can be mitigated by network planning and optimization methods. Implementation of such methods would be more practical for macrocell deployment compared, since small cell deployments are random and in mass amount. Therefore, we can say that macrocell cooperation with dense small cells gives a huge performance advantages for mobility issues and network planning.

TABLE III
Handover performance

Case	HO rate [HOs/sec/user]	HO failure rate [Fails/HO]	HO failure [Fails/sec/user]
Macrocell, 3km/h, Center	0.0058	0.001	5.8 x10^{-6}
Macrocell, 3km/h, Corner	0.0054	0.14	756 x10^{-6}
Macrocell, 50km/h, Center	0.0662	0.03	1986 x10^{-6}
Macrocell, 50km/h, Corner	0.0644	0.25	16600 x10^{-6}
Small cell, 3km/h	0.0131	0.06	786 x10^{-6}
Small cell, 50km/h	0.1478	0.45	66510 x10^{-6}

References

[1] T. Nakamura, S. Nagata, A. Benjebbour, Y. Kishiyama, T. Hai, S. Xiaodong, Y. Ning, and L. Nan, "Trends in small cell enhancements in LTE advanced," *IEEE Commun. Mag.*, vol. 51, no. 2, pp. 98–105, 2013.

[2] 3GPP, RWS-120045, *Summary of 3GPP TSG-RAN Workshop on Releae 12 and Onward.*, Jun. 2012.

[3] 3GPP TR 36.932 V12.1.0, *Scenarios and requirements for small cell enhancements for E-UTRA and E-UTRAN.*, Mar. 2013. [Online]. Available: http://www.3gpp.org/ftp/Specs/html-info/36932.htm

[4] J.-E. Berg, "A recursive method for street microcell path loss calculations," in *Proc. IEEE Int. Symp. on Personal, Indoor and Mobile Radio Comm.*, vol. 1, 1995, pp. 140–143.

[5] S. Parkvall, E. Dahlman, G. Jöngren, S. Landström, and L. Lindbom, "Heterogeneous network deployments in LTE - the soft-cell approach," *Ericsson review*, 2011.

[6] H. Ishii, Y. Kishiyama, and H. Takahashi, "A novel architecture for LTE-B: C-plane/U-plane split and Phantom Cell concept," in *Proc. IEEE Globecom Wksp.*, Dec. 2012, pp. 624–630.

[7] M. Gudmundson, "Cell planning in manhattan environments," in *Proc. IEEE Veh. Tech. Conf.*, 1992, pp. 435–438 vol.1.

[8] P. E. Ostling, "Implications of cell planning on handoff performance in manhattan environments," in *Proc. IEEE Int. Symp. on Personal, Indoor, and Mobile Radio Comm.*, 1994, pp. 625–629 vol.2.

[9] "Guidelines for evaluation of radio interface technologies for IMT-Advanced," ITU-R M.2135, Tech. Rep., 2008.

[10] H. Jamshid, "CDMA uplink power control methodology in SEAMCAT (voice only)," *CEPT WGSE PT SE21, QUALCOMM*, 2003.